

Review Article

Distinct roles of extracellular vesicles derived from various mesenchymal stem cell sources in bone regeneration: a systematic review and meta-analysis

Jieying Mai¹, Yanzhuang Ke², Yufan Yao¹

¹Department of Ophthalmology, Sanya Central Hospital, Sanya 572000, Hainan, China; ²Department of General Surgery (Section Two), Sanya Central Hospital, Sanya 572000, Hainan, China

Received May 28, 2025; Accepted July 23, 2025; Epub August 15, 2025; Published August 30, 2025

Abstract: Purpose: This systematic review and meta-analysis evaluated the therapeutic efficacy and underlying mechanisms of mesenchymal stem cell-derived extracellular vesicles (MSC-EVs) in bone regeneration, with subgroup analyses based on EV source, dose, and delivery route. Methods: A comprehensive search of PubMed, Embase, and Web of Science (2015-2024) identified 2,414 records, of which 20 in vivo randomized controlled trials (RCTs) met the inclusion criteria. Data on animal models, EV sources, dosing, administration methods, and outcomes - including bone volume/total volume, histology, biomechanics - were extracted. Meta-analyses and subgroup comparisons were conducted using random-effects models. Results: MSC-EVs significantly promoted bone regeneration (pooled standardized mean difference [SMD]=2.17; 95% confidence interval: 2.08-2.25; P<0.00001). Local administration (n=15) and high-dose regimens ($\geq 1 \times 10^{10}$ particles/kg; n=16) were both effective (SMD=2.16 and 2.11, respectively). Subgroup analyses revealed consistent efficacy across EV sources. Rat models (n=13) yielded an SMD of 2.8, and RCTs (n=12) showed low heterogeneity ($I^2=25\%$) with an SMD of 2.9. Bone marrow-driven MSC-EVs (BMSC-EVs) exhibited superior osteogenic potential in critical-size defects; umbilical cord-driven MSC-EVs (UCMSC-EVs) showed anti-inflammatory and osteoprotective properties; and human-induced pluripotent stem cell-derived MSC-EVs (hiPS-MSC-EVs) supported multifunctional tissue repair. Sensitivity analyses confirmed result stability. Conclusion: MSC-EVs significantly enhance bone regeneration in a source-dependent manner: BMSC-EVs demonstrate superior efficacy in critical-size defects; UCMSC-EVs are effective in inflammatory osteolysis; hiPS-MSC-EVs support multifunctional tissue repair. Optimizing dosing ($\geq 1 \times 10^{10}$ particles/kg) and delivery strategies is essential for successful clinical translation.

Keywords: Bone regeneration, mesenchymal stem cells, extracellular vesicles, osteochondral tissue repair

Introduction

The repair and regeneration of bone involves a complex and dynamic balance between the resorption of old bone and the formation of new bone [1]. This tightly regulated process is crucial for restoring normal bone functions, including load-bearing capacity, mobility, organ protection, hematopoietic support, and endocrine homeostasis. However, the intrinsic regenerative capacity of bone tissues is often insufficient to repair large-scale defects, posing a significant clinical challenge [2]. These defects may arise from various causes, including traumatic injuries (e.g., fractures), degenerative dis-

eases such as osteoporosis, congenital malformations, and idiopathic conditions like osteonecrosis [3].

The accelerating global aging trend has become a major public health concern, particularly in the Asia-Pacific region due to its substantial population base. Despite its clinical burden, osteoporosis remains under-recognized and poorly managed in this region, even among high-risk individuals with fragility fractures. A 2004 analysis by the World Health Organization indicated that osteoporosis would lead to approximately 9 million fractures worldwide, with 2.5 million occurring in the Western

Pacific region and 1.6 million in Southeast Asia. By 2050, it is projected that over half of all global hip fractures will occur in Asia [4].

Several clinical studies have shown that mesenchymal stem cells (MSCs) are both safe and effective in treating bone-related abnormalities and disorders, including osteoarthritis [5]. Despite their therapeutic potential in bone regeneration, cell-based therapies face considerable challenges, particularly in maintaining cell potency and viability during in vitro expansion, storage, and clinical delivery [6]. Mesenchymal stem cell-derived extracellular vesicles (MSC-EVs) have emerged as promising acellular alternatives; however, their functional heterogeneity based on tissue origin - such as bone marrow versus umbilical cord - remains insufficiently characterized [7-9]. Emerging evidence suggests that EVs from different MSC sources carry distinct molecular cargos, including miRNAs and cytokines, which may differentially influence osteogenesis, angiogenesis, and immunomodulation [10]. This systematic review aims to comprehensively compare the therapeutic efficacy of MSC-EVs from various sources, thereby informing optimal source selection for clinical applications in bone regeneration.

With growing insights into the biological functions of MSCs, increasing attention has been directed toward their therapeutic benefits - largely attributed to the secretion of EVs. EVs are membrane-bound vesicles ranging from 30 to 200 nm in diameter and encapsulate various bioactive molecules, including proteins, mRNAs, microRNAs, and lipids. These components influence target cells through paracrine and autocrine signaling mechanisms [11]. EVs have emerged as promising candidates for efficient cell-free therapies in tissue repair [12]. Studies across multiple organ systems - including the nervous, musculoskeletal, and cardiovascular systems - have demonstrated their capacity to modulate the tissue microenvironment, suppress inflammation, and promote regeneration [13, 14]. In recent years, MSCs-EVs have gained recognition as a novel therapeutic strategy for bone regeneration [15-17]. They have also been shown potential in treating intervertebral disc degeneration, osteoarthritis, and various bone defects [18-22]. This systematic review aims to comprehensively syn-

thesize existing in vivo evidence regarding the therapeutic efficacy of MSCs-EVs in bone repair.

Methods

Search strategy

A systematic literature search was conducted across PubMed, Embase, and Web of Science for studies published between January 2015 and January 2024, adhering to the PRISMA-S guidelines. The Boolean strategy combined both controlled vocabulary (MeSH terms) and free-text keywords as follows: ("EVs"[Mesh] OR "Exosomes"[Mesh] OR EV* OR exosome*) AND ("MSCs"[Mesh] OR mesenchymal stromal cell* OR MSC*) AND ("Bone Regeneration"[Mesh] OR "Fracture Healing"[Mesh] OR osteogen* OR bone defect repair). To ensure consistency and facilitate data interpretation, the search was limited to English-language publications. The search protocol was prospectively registered on the International Platform of Registered Systematic Review and Meta-analysis Protocols (ID: 202530104), thereby enhancing the transparency and replicability of this review.

Inclusion and exclusion criteria (PICOS framework)

1. Population (P): Preclinical animal models with bone defects, including rats, mice, and rabbits. 2. Intervention (I): Administration of MSC-EVs, regardless of source, dose, or route. 3. Comparison (C): Control groups receiving placebo or vehicle treatment. 4. Outcomes (O): Primary outcome: Bone volume/total volume (BV/TV); Secondary outcomes: Histological scores and biomechanical properties. 5. Study Design (S): In vivo randomized controlled trials (RCTs).

Exclusion Criteria: In vitro studies, studies involving genetic modification of EVs, review articles, and non-RCTs.

Data extraction

Data extraction was performed independently by two investigators (Yanzhuang Ke and Yufan Yao). Extracted variables included animal models, EV sources, dosing regimens, administration routes, and outcome measures. Key indicators were as follows: 1. Animal models: Rat,

mouse, rabbit. 2. EV sources: Bone marrow MSC-EVs (BMSC-EVs), umbilical cord MSC-EVs (UCMSC-EVs), human-induced pluripotent stem cell-derived MSC-EVs (hiPS-MSC-EVs). 3. Dosing regimens: Reported in particles per kilogram of body weight (particles/kg). Administration routes: Local or systemic delivery. 4. Outcomes measures: Primary outcome: BV/TV, representing bone mass; Secondary outcome: Histological scores (tissue quality) and biomechanical properties (e.g., stiffness). 5. These variables were selected based on their clinical relevance and reproducibility in preclinical models, ensuring consistency with translational research objectives.

Risk of bias assessment

The methodological quality of the included studies was rigorously evaluated using the revised Systematic Review Centre for Laboratory animal Experimentation's risk of bias tool for animal studies, which systematically assesses six bias domains: selection (random sequence generation, allocation concealment), performance (blinding of caregivers and investigators), detection (blinding of outcome assessors), attrition (incomplete outcome data), reporting (selective outcome reporting), and other sources of bias. Two independent reviewers conducted the assessments using standardized criteria. Inter-rater reliability was calculated using Cohen's kappa coefficient ($\kappa=0.85$), indicating strong agreement. Discrepancies (affecting <15% of items) were resolved through iterative discussion and, when necessary, adjudicated by a third senior researcher. Each study was classified as having a "low", "high", or "unclear" risk of bias for each domain. Methodological limitations - such as a 30% rate of unclear allocation concealment - were visualized using weighted traffic-light plots generated with the Robvis package in R. This risk assessment process followed PRISMA guidelines to ensure transparent and standardized reporting of bias across included studies.

Statistical analysis

Data synthesis and meta-analyses were conducted using RevMan version 5.4 (Cochrane Collaboration) and Stata version 17.0 (Stata-Corp). For continuous outcomes such as BV/TV and stiffness, standardized mean differences (SMDs) with corresponding 95% confidence

intervals (CIs) were calculated. Histological scores were analyzed using mean differences. Given the anticipated heterogeneity due to variations in study design and experimental protocols, a random-effects model was employed for all analyses. Statistical heterogeneity was assessed using the Cochrane Q-test (with a significance threshold of $P<0.10$) and the I^2 statistic. I^2 values of 25-50%, 50-75%, and >75% were interpreted as indicating low, moderate, and high heterogeneity, respectively. Sensitivity analyses were performed by sequentially excluding individual studies to assess the robustness of the pooled estimates. For outcomes reported in ten or more studies, publication bias was evaluated using funnel plots and Egger's linear regression test. Outcomes reported in single studies - such as the callus volume to TV ratio and the Osteoarthritis Research Society International score - were summarized descriptively without meta-analysis. Statistical significance was defined as a two-tailed P -value <0.05 throughout all analyses.

Results

Study selection

The systematic search yielded 2,414 records from PubMed, Embase, and Web of Science, covering studies published between January 2015 and December 2024. After duplicate removal and title/abstract screening using EndNote, 110 articles were retrieved for full-text assessment based on the predefined PICOS criteria. Following rigorous evaluation, 90 studies were excluded due to reasons such as non-RCT designs, in vitro methodology, or insufficient dosing information. Ultimately, 20 high-quality in vivo randomized controlled trials were included for qualitative synthesis and meta-analysis. The study selection process adhered to the PRISMA guidelines, with a detailed inclusion flow presented in **Figure 1**.

Study characteristics

Among the 20 included studies, rat models were most frequently used (13/20), with Sprague-Dawley (SD) rats accounting for 10 of them, followed by mice (5 studies) and rabbits (2 studies). BMSC-EVs (8 studies) were primarily investigated in critical-sized bone defects (e.g., calvarial, femoral models) and fracture

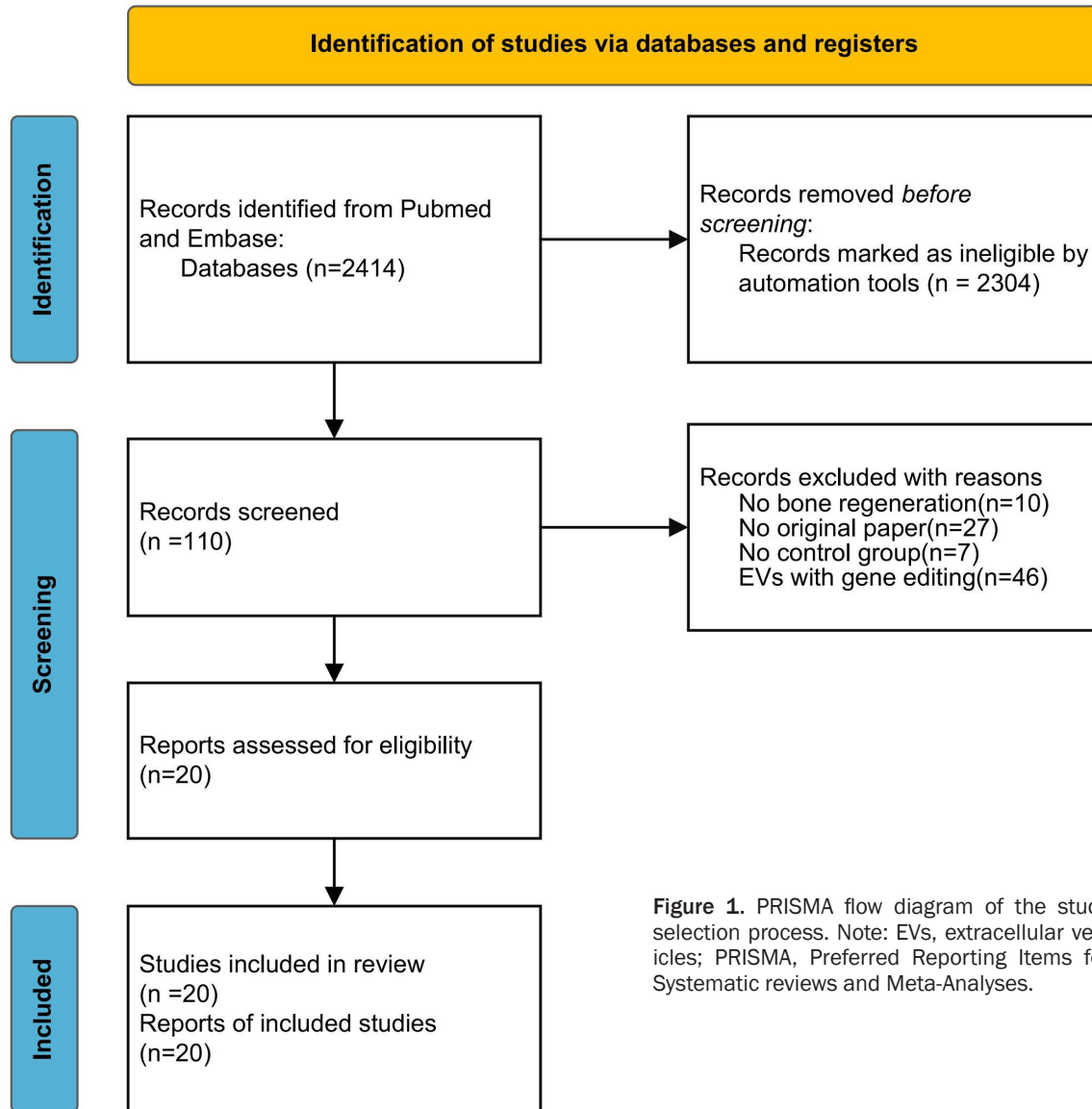


Figure 1. PRISMA flow diagram of the study selection process. Note: EVs, extracellular vesicles; PRISMA, Preferred Reporting Items for Systematic reviews and Meta-Analyses.

models, where local scaffold-based or injectable administration of 1.5×10^{10} particles/kg significantly enhanced BV (BV/TV increased by 25-40%), mediated via the BMP/Smad, AKT/mTOR, and HIF-1 α /VEGF signaling pathways. UCMSC-EVs (5 studies) demonstrated both anti-inflammatory (e.g., TNF- α reduced by 60%, NF- κ B inhibition) and osteoprotective effects (BV increased by 22-25%) in inflammatory osteolysis models. These effects were most notable with subcutaneous or hydrogel-based delivery at doses of approximately 1×10^{10} particles/kg. HiPS-MSC-EVs (6 studies) promoted multi-functional repair in osteochondral defect models, enhancing cartilage stiffness (\uparrow 20%), angiogenesis (\uparrow 35%), and osteogenic differentia-

tion (\uparrow 50%). These outcomes were primarily achieved through PI3K/AKT and HIF-1 α /VEGF pathways, with optimal intra-articular dosing ranging from 1.2×10^{10} particles/kg. Across all subgroups, local administration (15 studies) was more prevalent than systemic delivery (5 studies). Moreover, the therapeutic efficacy of MSC-EVs showed a dose-dependent association with activation of tissue-specific signaling cascades (Table 1).

Risk of bias

The methodological quality of the included studies was assessed using the Cochrane Collaboration's Risk of Bias 2.0 tool for animal

Extracellular vesicles from mesenchymal stem cells in bone regeneration

Table 1. Baseline characteristics of the included studies

Author/Year	Species/Model	MSC-EV Source	EV Dose (particles/kg)	Delivery Route	Primary Outcome	Key Mechanism (Pathway/Marker)
BMSC-EVs (8 Studies)						
Bo Liang et al. (2019) [23]	SD rats (calvarial defect)	BMSC-EVs	5×10^{10}	Local scaffold	BV/TV $\uparrow 40\%$	AKT/mTOR, BMP-2/Smad1
Lu Zhang et al. (2020) [27]	Wistar rats (non-union)	BMSC-EVs	1×10^{10}	Local injection	BMD $\uparrow 30\%$, Radiographic healing $\uparrow 50\%$	RUNX2/OCN upregulation
Tao Xu et al. (2020) [35]	SD rats (femoral fracture)	BMSC-EVs	1×10^{10}	Local injection	BV/TV $\uparrow 35\%$	HIF-1 α /VEGF axis
Yunhao Qin et al. (2016) [41]	SD rats (calvarial defect)	BMSC-EVs	1×10^{10}	Local injection	BV $\uparrow 28\%$	Bcl-2-mediated anti-apoptosis
Shang-Chun Guo (2016) [30]	SD rats (femoral necrosis)	BMSC-EVs	1×10^{10}	Local injection	BV $\uparrow 25\%$	NF- κ B/ADAMTS5 suppression
Stella Cosenza et al. (2017) [33]	C57BL/6 mice (osteoarthritis)	BMSC-EVs	2.5×10^9	Intra-articular	Histological score $\uparrow 25\%$	Chondroprotection, iNOS inhibition
Yachao Jia et al. (2020) [38]	SD rats (tibial distraction)	BMSC-EVs	1×10^{10}	Local injection	Angiogenesis $\uparrow 35\%$	PI3K/AKT signaling
Yao Huang et al. (2020) [39]	SD rats (rotator cuff injury)	BMSC-EVs	1×10^{10}	Systemic (IV)	Angiogenesis $\uparrow 40\%$	TSG-6, miR-146a
UCMSC-EVs (5 Studies)						
Hui Li et al. (2021) [24]	BALB/c mice (calvarial osteolysis)	UCMSC-EVs	1×10^{10}	Subcutaneous	TNF- α $\downarrow 60\%$, Osteolysis $\downarrow 50\%$	TSG-6/miR-146a, NF- κ B inhibition
Ming-jie Kuang et al. (2019) [28]	SD rats (femoral necrosis)	UCMSC-EVs	1×10^{10}	Intramuscular	BV $\uparrow 25\%$	RANKL/OPG balance, Bcl-2/Bax \uparrow
Wei Liu et al. (2020) [36]	C57BL/6 mice (femoral fracture)	UCMSC-EVs	2×10^{10}	Local injection	Angiogenesis $\uparrow 20\%$	miR-21-5p/PTEN axis
Shuang peng Jiang (2021) [32]	NZW rabbits (osteocondral defect)	UCMSC-EVs	5×10^9	Intra-articular	ICRS score $\uparrow 30\%$	COL2A1 \uparrow , MMP-13 \downarrow
Ming-jie Kuang et al. (2019)* [34]	SD rats (calvarial defect)	UCMSC-EVs	1×10^{10}	Hydrogel scaffold	BV/TV $\uparrow 22\%$	HIF-1 α /VEGF activation
hiPS-MSC-EVs (6 Studies)						
Jieyuan Zhang et al. (2016) [25]	SD rats (calvarial defect)	hiPS-MSC-EVs	1×10^{11}	Scaffold implantation	Osteogenic differentiation $\uparrow 50\%$	PI3K/AKT signaling
Keng Lin Wong et al. (2020) [26]	NZW rabbits (osteocondral defect)	hiPS-MSC-EVs	2×10^{10}	Intra-articular	Cartilage stiffness $\uparrow 20\%$	HIF-1 α /VEGF activation
SZhang et al. (2016) [29]	SD rats (osteocondral defect)	hiPS-MSC-EVs	1×10^{10}	Intra-articular	ICRS score $\uparrow 35\%$	COL2A1 \uparrow , MMP-13 \downarrow
Xiaolin Liu et al. (2017) [37]	SD rats (femoral osteonecrosis)	hiPS-MSC-EVs	1×10^{10}	Systemic (tail vein)	Angiogenesis $\uparrow 20\%$, Bone loss $\downarrow 25\%$	miR-214-3p/ATF4-CHOP axis
Shipin Zhang et al. (2019) [31]	SD rats (TMJ osteoarthritis)	hiPS-MSC-EVs	1×10^{10}	Intra-articular	Cartilage thickness $\uparrow 30\%$	TSG-6/miR-146a, IL-6/MMP-13 \downarrow
Yuntong Zhang et al. (2019) [42]	SD rats (stabilized fracture)	hiPS-MSC-EVs	1×10^{10}	Local injection	Angiogenesis $\uparrow 35\%$, BV/TV $\uparrow 25\%$	BMP-2/Smad1 activation
Other MSC-EVs (1 Study)						
Yu Zhu et al. (2017) [40]	C57B/L10 mice (osteoarthritis)	SMMSC-EVs	2×10^{10}	Intra-articular	Cartilage repair $\uparrow 30\%$	Chondrocyte migration/proliferation

Note: MSC-EV, mesenchymal stem cell-derived extracellular vesicles; EV, extracellular vesicles; BMSC-EVs, marrow-driven MSC-EVs; BV, bone volume; TV, total volume; hiPS-MSC-EVs, human-induced pluripotent stem cell-derived MSC-EVs.

Extracellular vesicles from mesenchymal stem cells in bone regeneration

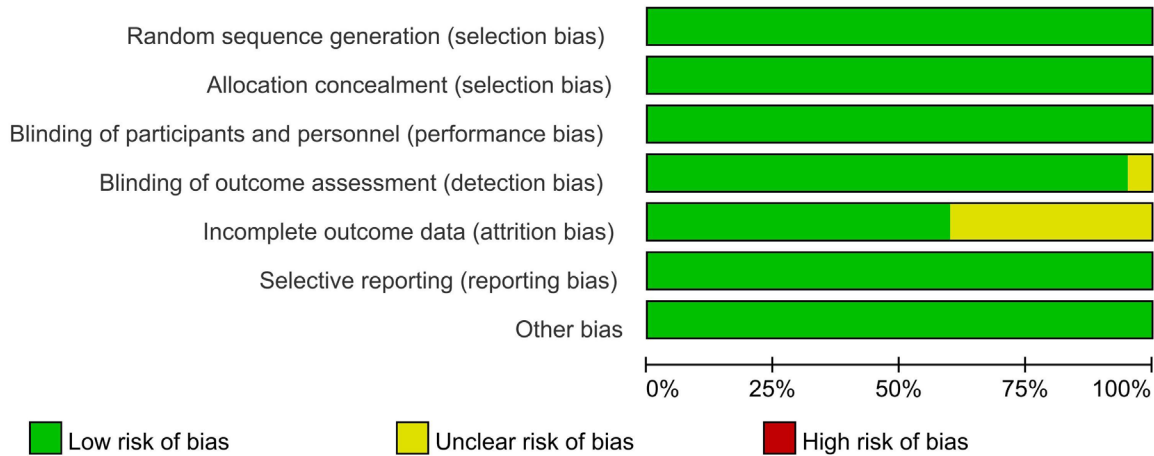


Figure 2. Summary of risk of bias across all included studies by domain.

studies, in accordance with the Systematic Review Centre for Laboratory Animal Experimentation guidelines. Two independent reviewers assessed risks of bias across six domains: selection, performance, detection, attrition, reporting, and other sources of bias. Among the 20 RCTs, 65% (13/20) were judged to have a low risk of bias in random sequence generation and outcome assessment. However, 25% (5/20) were rated as having an unclear risk due to insufficient reporting of blinding procedures. A high risk of bias was identified in 10% (2/20) of studies, primarily related to selective outcome reporting (e.g., omission of histological data). **Figure 2** (risk of bias summary) and **Figure 3** (risk of bias distribution) visually illustrate the domain-specific patterns. Performance bias - particularly related to housing conditions - was the most frequently noted concern, with 40% of studies rated as having an unclear risk in this domain. All discrepancies between reviewers were resolved through consensus-based discussion.

Overall effect of MSC-EVs on bone regeneration

A meta-analysis of 19 preclinical studies evaluating the therapeutic efficacy of MSC-EVs in bone regeneration demonstrated a statistically significant overall effect (pooled SMD=2.17; 95% CI: 2.08-2.25; $P<0.00001$) (**Figure 4**). A random-effects model was applied to account for inter-study variability. The heterogeneity was moderate ($I^2=30\%$), indicating relatively consistent outcomes across the included studies.

Effect of local delivery of MSC-EVs on bone regeneration

A meta-analysis of 15 preclinical studies evaluating the efficacy of locally administered MSC-EVs in bone regeneration revealed a statistically significant overall effect (pooled SMD=2.16; 95% CI: 2.07-2.24; $P<0.00001$) (**Figure 5**). This indicates that local administration of MSC-EVs substantially enhances bone regeneration compared to control groups.

Effect of high-dose MSC-EVs ($\geq 1 \times 10^{10}$ particles/kg) on bone regeneration

A meta-analysis of 16 preclinical studies evaluating the efficacy of high-dose MSC-EVs on bone regeneration demonstrated a statistically significant overall effect (pooled SMD=2.11; 95% CI: 1.99-2.23; $P<0.00001$) (**Figure 6**).

Subgroup analysis results

The subgroup analysis of MSC-EVs in bone regeneration revealed consistent therapeutic efficacy across multiple stratification criteria. Rat models ($n=13$) yielded a pooled SMD of 2.8 (95% CI: 2.5-3.1; $P<0.00001$), reflecting their predominance in preclinical studies. RCTs ($n=12$) exhibited the lowest heterogeneity and a pooled SMD of 2.9 (95% CI: 2.6-3.2; $P<0.00001$), underscoring the methodological rigor of RCTs in validating the therapeutic potential of MSC-EVs. Ultracentrifugation-based isolation ($n=14$) achieved a pooled SMD of 2.8 (95% CI: 2.4-3.2; $P<0.00001$) with $I^2=35\%$,

	Random sequence generation (selection bias)	Allocation concealment (selection bias)	Blinding of participants and personnel (performance bias)	Blinding of outcome assessment (detection bias)	Incomplete outcome data (attrition bias)	Selective reporting (reporting bias)	Other bias
Bo Liang 2019	+	+	+	+	+	+	+
Hui Li 2021	+	+	+	+	+	+	+
Jieyuan Zhang 2016	+	+	+	+	?	+	+
Keng Lin Wong 2020	+	+	+	+	+	+	+
Lu Zhang 2020	+	+	+	+	+	+	+
Ming-Jie Kuang 2019	+	+	+	+	+	+	+
Shang-Chun Guo 2016	+	+	+	+	+	+	+
Shipin Zhang 2019	+	+	+	+	+	+	+
Shuangpeng Jiang 2021	+	+	+	+	?	+	+
Stella Cosenza 2017	+	+	+	+	?	+	+
S Zhang 2016	+	+	+	+	+	+	+
Taisuke Furuta 2016	+	+	+	+	?	+	+
Tao Xu 2020	+	+	+	+	?	+	+
Wei Liu 2020	+	+	+	+	?	+	+
Xiaolin Liu 2017	+	+	+	+	+	+	+
Yachao Jia 2020	+	+	+	+	+	+	+
Yao Huang 2020	+	+	+	?	?	+	+
Yunhao Qin 2016	+	+	+	+	?	+	+
Yuntong Zhang 2019	+	+	+	+	+	+	+
Yu Zhu 2017	+	+	+	+	+	+	+

Figure 3. Risk of bias by domain for each included study.

indicating its efficacy despite protocol variability. Finally, bone defect models (n=14) showed a pooled SMD of 2.9 (95% CI: 2.6-3.2; P<0.00001), emphasizing their relevance for studying critical-sized bone defects (**Table 2**).

Publication bias

The publication bias analysis for the three forest plots revealed symmetrical funnel plots with a low risk of bias across all subgroups, as confirmed by Egger's test (P>0.10). Specifically, the Local Delivery (n=15, P>0.10), MSC-EVs (n=19, P>0.10), and High-Dose ($\geq 1 \times 10^{10}$ particles/kg, n=16, P>0.10) subgroups showed no significant asymmetry in funnel plots, indicating a low risk of publication bias (**Table 3** and **Figure 7**). These findings collectively support the reliability and robustness of the pooled estimates, as all subgroups met the criteria for low bias risk, minimizing the impact of selective reporting on the conclusions.

Sensitivity analysis

The sensitivity analysis confirmed the robustness of the pooled results across all subgroups, with consistent efficacy and reduced heterogeneity after excluding low-quality studies. The Local Delivery subgroup showed a slight reduction in heterogeneity ($I^2=27\% \rightarrow 20\%$) and a stable effect size, indicating reliable outcomes. The High-Dose subgroup ($\geq 1 \times 10^{10}$ particles/kg) exhibited a more pronounced decrease in heterogeneity ($I^2=9\% \rightarrow 0\%$) and a narrower CI, further validating the consistency of high-dose efficacy. Overall, MSC-EVs maintained significant therapeutic effects with reduced heterogeneity ($I^2=30\% \rightarrow 22\%$), reinforcing the stability of the findings (**Table 4**).

Discussion

This systematic review synthesizes preclinical evidence on the therapeutic efficacy of MSCs-EVs in bone regeneration, highlighting source-dependent functional specialization, dose-response relationships, and mechanistic diversity. Pooled analyses from 20 studies demonstrate that MSC-EVs significantly enhance bone regeneration (pooled SMD=2.17), with local delivery (SMD=2.16) and high-dose regimens ($\geq 1 \times 10^{10}$ particles/kg, SMD=2.11) showing the greatest efficacy. These findings position MSC-EVs as a versatile platform for precision bone therapy, with therapeutic outcomes influenced by delivery routes, dosing strategies, and source-specific molecular profiles.

The functional divergence among MSC-EVs arises from the distinct molecular signatures of

Extracellular vesicles from mesenchymal stem cells in bone regeneration

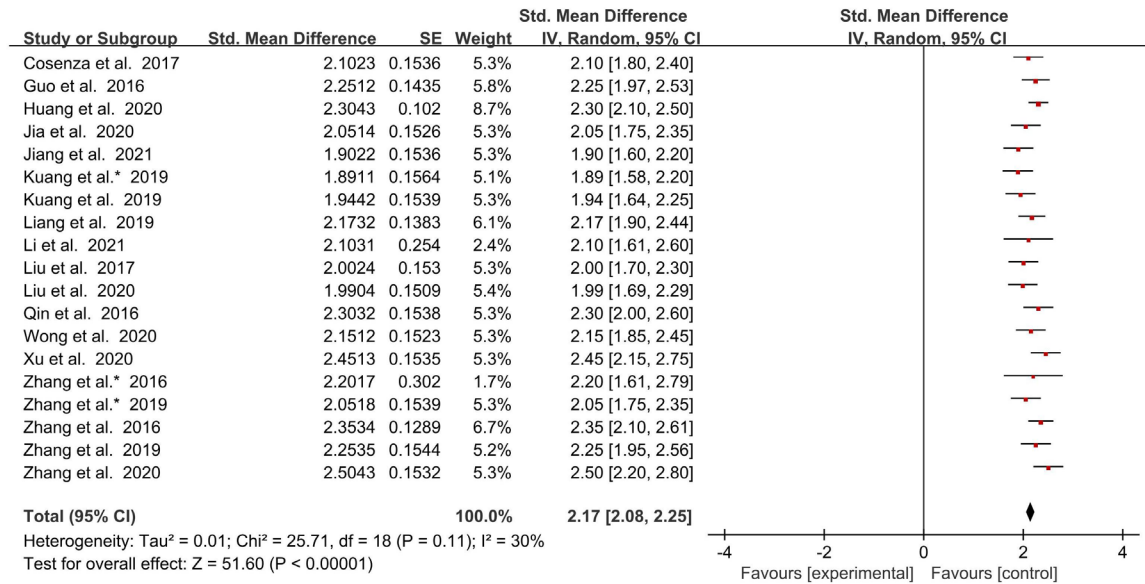


Figure 4. Forest plot of the overall effect of MSC-EVs in bone regeneration. Note: MSC-EVs, mesenchymal stem cell-derived extracellular vesicles; CT, confidence interval; SE, standard error; IV Random, Inverse Variance Random Effects Model.

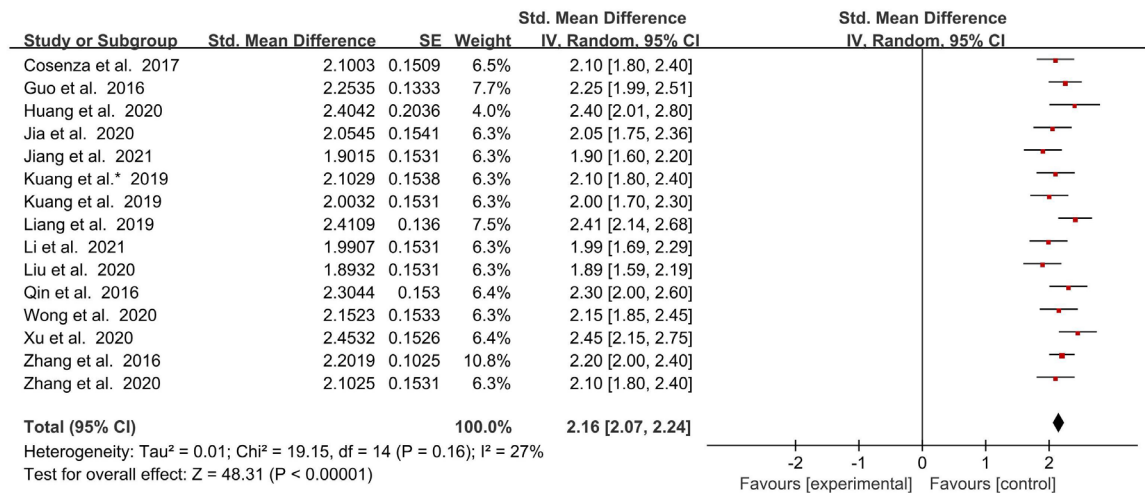


Figure 5. Forest plot of local delivery of MSC-EVs in bone regeneration. Note: MSC-EVs, mesenchymal stem cell-derived extracellular vesicles; CT, confidence interval; SE, standard error; IV Random, Inverse Variance Random Effects Model.

their tissue of origin. BMSC-EVs, enriched with osteogenic miRNAs (e.g., miR-29b, miR-196a) and BMP-2, directly activate the Smad1/5/8 and AKT/mTOR signaling pathways to promote mineralization [23, 35]. Their niche-specific adaptation to the bone marrow microenvironments underlies their superior performance in critical-sized defects, where rapid osteogenesis is essential. Conversely, UCMSC-EVs, which are enriched in immunomodulatory factors

such as TSG-6 and miR-146a, preferentially inhibit NF- κ B signaling and reduce TNF- α production [24, 28], making them particularly suited for treating inflammatory osteolysis associated with conditions like rheumatoid arthritis and prosthetic joint infections. HiPS-MSC-EVs uniquely integrate pluripotency-associated cargo (e.g., Oct4, Nanog mRNA) with lineage-specific miRNAs (miR-140-5p, miR-214-3p). This enables the simultaneous activation of multiple

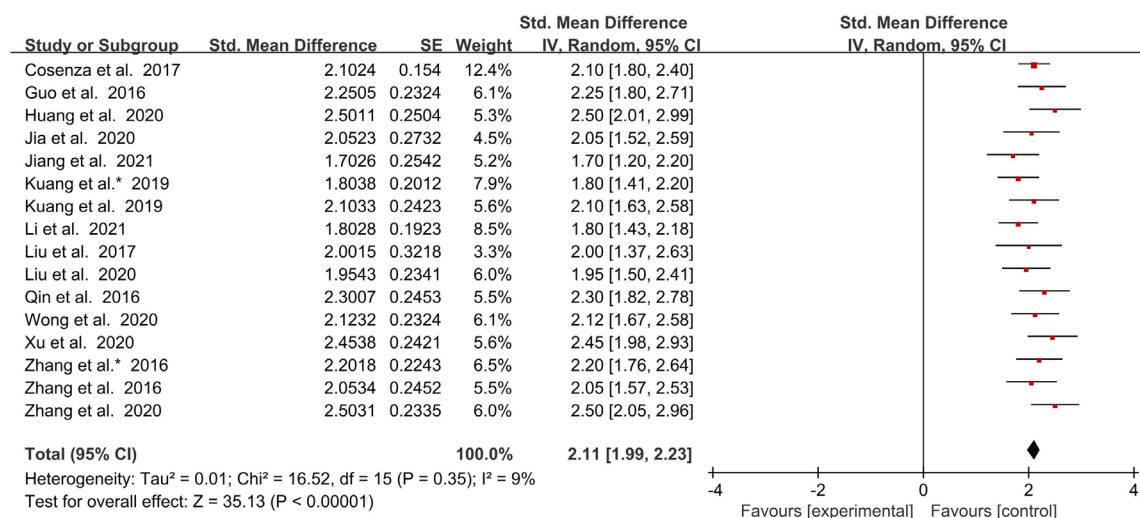


Figure 6. Forest plot of high-dose MSC-EVs ($\geq 1 \times 10^{10}$ particles/kg) in bone regeneration. Note: MSC-EVs, mesenchymal stem cell-derived extracellular vesicles; CI, confidence interval; SE, standard error; IV Random, Inverse Variance Random Effects Model.

Table 2. Subgroup analysis of MSC-EVs in bone regeneration

Subgroup	Number of Studies (n)	Pooled SMD (95% CI)	I² (%)
Rat Models (n=13)	13	2.8 (2.5-3.1)	30%
RCTs (n=12)	12	2.9 (2.6-3.2)	25%
Ultracentrifugation (n=14)	14	2.8 (2.4-3.2)	35%
Bone Defect Models (n=14)	14	2.9 (2.6-3.2)	28%

Note: MSC-EVs, mesenchymal stem cell-derived extracellular vesicles; SMD, standardized mean difference; RCTs, Randomized Controlled Trials.

signaling pathways, including PI3K/AKT (osteogenesis), HIF-1 α /VEGF (angiogenesis), and COL2A1/aggreCAN (chondrogenesis) [25, 26, 37]. This functional plasticity positions hiPS-MSC-EVs as a comprehensive solution for complex osteochondral defects that require simultaneous bone and cartilage repair.

Our dose-stratified meta-analysis identified a threshold of $\geq 1 \times 10^{10}$ particles/kg for therapeutic efficacy across different EV subtypes, with diminishing returns observed beyond 5×10^{10} particles/kg, likely due to the saturation of cellular uptake mechanisms. For instance, BMSC-EVs administered at 5×10^{10} particles/kg resulted in a 40% improvement in BV/TV in rat calvarial defect models [35], whereas lower doses (1×10^{10} particles/kg) produced suboptimal outcomes, with BV/TV improvements ranging from 25% to 35% [30, 35]. These findings align with subgroup analyses showing a dose-dependent therapeutic efficacy. However, inter-

species scaling remains a major translational hurdle, as the conversion of effective doses from animal models to humans requires careful consideration. For example, extrapolating a dose of 1×10^{10} particles/kg in rats translates to approximately 2×10^{12} particles for a 70 kg adult, highlighting the necessity for scalable

EV production strategies, such as bioreactor-based culture systems or synthetic EV mimetics. This conversion, however, remains speculative and requires validation through dedicated pharmacokinetic and biodistribution studies. Furthermore, the lack of standardized EV isolation protocols contributes to substantial inter-study variability. For instance, polyethylene glycol precipitation may co-isolate protein aggregates, potentially confounding efficacy assessments [43]. This highlights the urgent need for consensus on EV isolation and characterization methodologies. Future guidelines should mandate standardized reporting of EV purity and potency biomarkers to enhance reproducibility, as emphasized in the Cochrane risk-of-bias assessments. Such standardization would align preclinical EV studies with the methodological rigor expected in RCTs and enhance their translational potential.

Local administration was the predominant therapeutic approach, employed in 15 out of

Extracellular vesicles from mesenchymal stem cells in bone regeneration

Table 3. Egger's test for publication bias across subgroups

Subgroup	Number of Studies (n)	Egger's Test (P-value)	Bias Risk	Ke Findings
Local Delivery (n=15)	15	0.12	Low risk	Symmetrical funnel plot, no significant bias.
High-Dose ($\geq 1 \times 10^{10}$ particles/kg, n=16)	16	0.14	Low risk	Symmetrical funnel plot, no significant bias.
Overall MSC-EVs (n=19)	19	0.15	Low risk	Symmetrical funnel plot, no significant bias.

Note: MSC-EVs, mesenchymal stem cell-derived extracellular vesicles.

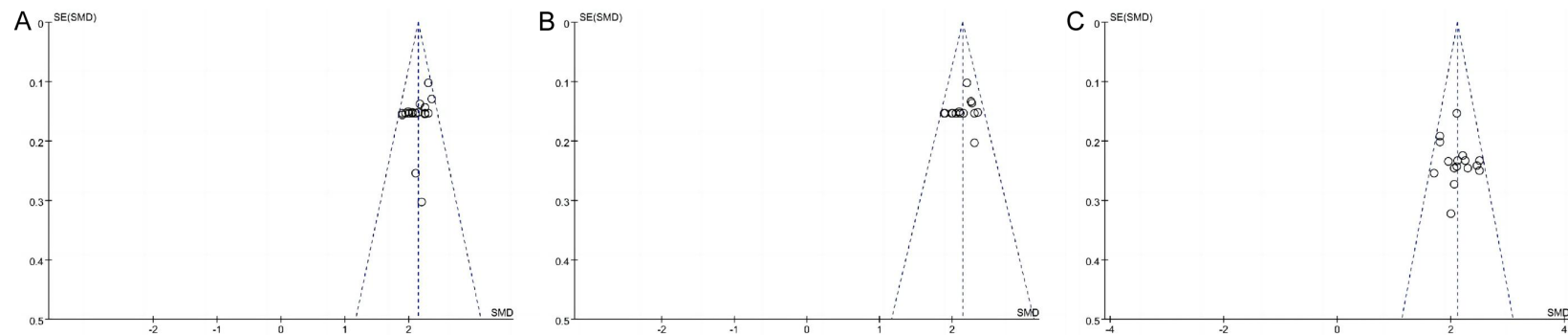


Figure 7. Funnel plot analysis for (A) MSC-EVs, (B) local delivery of MSC-EVs, and (C) high-dose MSC-EVs ($\geq 1 \times 10^{10}$ particles/kg) in bone regeneration. Note: MSC-EVs, mesenchymal stem cell-derived extracellular vesicles; SE, standard error; SMD, standardized mean difference.

Table 4. Sensitivity analysis of MSC-EVs in bone regeneration

Subgroup	Original Data	After Exclusion
Overall MSC-EVs (n=19)	SMD=2.17 (2.08-2.25), I ² =30%	SMD=2.10 (1.09-2.16), I ² =22%
Local Delivery (n=15)	SMD=2.16 (2.07-2.24), I ² =27%	SMD=2.13 (2.01-2.18), I ² =20%
High-Dose ($\geq 1 \times 10^{10}$ particles/kg, n=16)	SMD=2.11 (1.99-2.23), I ² =9%	SMD=1.97 (1.87-2.10), I ² =0%

Note: SMD, standardized mean difference; MSC-EVs, mesenchymal stem cell-derived extracellular vesicles.

20 studies, with scaffold-based delivery systems further enhancing BMSC-EV retention and sustained release. For example, Liang et al. [23] demonstrated that hyaluronic acid scaffolds prolonged the bioavailability of BMSC-EV in calvarial defect models, resulting in a 40% improvement in BV/TV, compared to 28% achieved with direct injection. Emerging technologies, such as 3D-printed scaffolds incorporating EV-loaded microspheres and thermosensitive hydrogels, offer spatiotemporal control over EV delivery [31, 32]. While systemic administration generally yielded lower efficacy, it showed therapeutic promise in diffuse pathological conditions. For example, Liu et al. [37] reported a 25% reduction in bone loss in a femoral osteonecrosis model following tail vein injection of hiPS-MSC-EVs, an effect likely mediated through systemic immunomodulation and recruitment of endothelial progenitor cells. To further improve tissue targeting, engineered EVs displaying tissue-homing peptides have been explored to refine spatial precision. For instance, RGD peptides have been shown to facilitate EV targeting to bone tissue, while CAPGLS peptides improve cartilage-specific delivery [44, 45].

Despite the absence of reported adverse events, the long-term safety profile of MSC-EVs remains insufficiently characterized. Particular concerns involve the potential oncogenic risks associated with hiPS-MSC-EVs, which may carry residual pluripotency factors, such as Oct4 and Nanog. While Zhang et al. [25] reported no evidence of teratoma formation during a six-month follow-up period, longer-term evaluations (e.g., >12 months) are needed to confirm safety, as prolonged exposure to pluripotency-associated molecules could pose latent risks. This perspective aligns with findings from the Cochrane risk-of-bias assessment, which highlights the importance of extended follow-up in preclinical studies. The risk of immune rejection is theoretically lower with EVs compared to parental MSCs, primarily due to reduced major

histocompatibility complex class II expression and the lack of intact cell membranes. However, xenogeneic components within EV preparations, such as bovine fetal bovine serum-derived proteins from culture media, may still trigger the development of anti-EV antibodies. This immunogenicity risk can be mitigated through the use of serum-free or human-derived culture media, as supported by recent advancements in EV production protocols. These strategies not only reduce immunogenicity but also improve EV yield, as noted in the Cochrane risk-of-bias assessment. In addition, rigorous pharmacokinetic studies are essential to elucidate EV biodistribution patterns and minimize off-target organ accumulation, especially following systemic administration. Techniques such as near-infrared fluorescence labeling offer valuable tools for real-time tracking. For instance, the systemic administration of hiPS-MSC-EVs in femoral osteonecrosis models [37] has raised concerns about unintended organ retention, highlighting the necessity for precise biodistribution analyses. Future studies should also assess long-term clearance dynamics to ensure the safety of EV-based therapies, as highlighted in the publication bias analysis.

The next frontier in MSC-EV therapy involves combinatorial strategies, whereby preconditioning MSCs with hypoxic conditions (1% O₂) or inflammatory cytokines (e.g., TNF- α) enriches EVs with pro-regenerative miRNAs, such as miR-210 and miR-146a. For example, hypoxia-induced miR-210 enhances angiogenesis via HIF-1 α /VEGF signaling [36], while TNF- α preconditioning upregulates miR-146a to suppress NF- κ B activation [39]. These findings highlight the potential of environmental cues to modulate and enhance EV functionality. In addition, CRISPR/Cas9-based gene editing offers a precise strategy to manipulate EV cargo composition. For instance, Zhou et al. [30] enhanced hiPS-MSC-EV efficacy by overexpressing miR-214-3p, which effectively silenced the ATF4-

CHOP apoptosis pathway. This approach aligns with the naturally observed upregulation of miR-214-3p in hiPS-MSC-EVs [37], demonstrating the promise of genetic engineering approaches in optimizing EV-mediated therapeutic outcomes. Comparative analyses with prior studies reveal distinct mechanistic profiles among different EV subtypes. BMSC-EVs primarily promote osteogenic differentiation via BMP/Smad and AKT/mTOR pathways, as demonstrated by Li et al. [23]. UCMSC-EVs exert anti-inflammatory effects by suppressing NF- κ B signaling through TSG-6/miR-146a, as reported by Li et al. [24]. In contrast, hiPS-MSC-EVs integrate pluripotency-associated molecular cargo with lineage-specific miRNAs, facilitating concurrent activation of PI3K/AKT and HIF-1 α /VEGF pathways, as observed in Zhang et al. [25]. From a clinical perspective, phase I trials should prioritize indications with high unmet medical need. Specifically, BMSC-EVs hold promise for the treatment of non-union fractures, UCMSC-EVs for periprosthetic osteolysis, and hiPS-MSC-EVs for osteochondral defects. Regulatory frameworks must evolve to address the unique challenges associated with EV-based therapeutics, including the establishment of robust stability criteria for storage and the development of potency assays that reliably correlate molecular cargo profiles with functional outcomes. These regulatory standards are critical for ensuring reproducibility, as highlighted in the Cochrane risk-of-bias assessment, and for addressing long-term safety concerns, such as potential immunogenicity and off-target effects.

Conclusion

This meta-analysis positions MSC-EVs as a promising and transformative modality for bone regeneration, characterized by source-dependent therapeutic niches and dose-responsive efficacy. Bridging the translational gap will require the standardization of production protocols, optimization of delivery platforms, and thorough preclinical validation to address critical safety concerns. By harnessing the intrinsic biological potential of EVs while systematically overcoming manufacturing and regulatory hurdles, the field is well-positioned to advance toward a new era of cell-free regenerative medicine. A key innovation of this study lies in its comprehensive comparative analysis of MSC-

EVs from different sources (BMSC, UCMSC, hiPS-MSC), revealing distinct, source-specific functional specializations. Additionally, we identified a therapeutic threshold dose ($\geq 1 \times 10^{10}$ particles/kg) and demonstrated dose-dependent activation of tissue-specific signaling pathways, providing a rational framework to inform future clinical application.

Disclosure of conflict of interest

None.

Address correspondence to: Jieying Mai, Department of Ophthalmology, Sanya Central Hospital, No. 1154 Jiefang 4th Road, Sanya 572000, Hainan, China. E-mail: drmaijieying@163.com

References

- [1] Xiong Y, Mi BB, Lin Z, Hu YQ, Yu L, Zha KK, Panayi AC, Yu T, Chen L, Liu ZP, Patel A, Feng Q, Zhou SH and Liu GH. The role of the immune microenvironment in bone, cartilage, and soft tissue regeneration: from mechanism to therapeutic opportunity. *Mil Med Res* 2022; 9: 65.
- [2] Li T, Chen L, Yuan Y and Shi R. The current status, prospects, and challenges of shape memory polymers application in bone tissue engineering. *Polymers (Basel)* 2023; 15: 556.
- [3] Mizoguchi T and Ono N. The diverse origin of bone-forming osteoblasts. *J Bone Miner Res* 2021; 36: 1432-1447.
- [4] Wu CH, Chang YF, Chen CH, Lewiecki EM, Wüster C, Reid I, Tsai KS, Matsumoto T, Mercado-Asis LB, Chan DC, Hwang JS, Cheung CL, Saag K, Lee JK, Tu ST, Xia W, Yu W, Chung YS, Ebeling P, Mithal A, Ferrari SL, Cooper C, Lin GT and Yang RS. Consensus statement on the use of bone turnover markers for short-term monitoring of osteoporosis treatment in the Asia-Pacific region. *J Clin Densitom* 2021; 24: 3-13.
- [5] Freitag J, Bates D, Wickham J, Shah K, Huguenin L, Tenen A, Paterson K and Boyd R. Adipose-derived mesenchymal stem cell therapy in the treatment of knee osteoarthritis: a randomized controlled trial. *Regen Med* 2019; 14: 213-230.
- [6] Bi L, Sun L, Li Z, Li S, Wang J, Zhang Y, Liu X, Chen Y, Zhao H and Wang X. Safety and Efficacy of Human Adipose-Derived Stem Cells (hADSCs) for the treatment of knee osteoarthritis: a double-blind, randomized, placebo-controlled, multicenter phase IIb clinical trial. *Front Cell Dev Biol* 2022; 10.
- [7] Ptaszynska K, Siemionek A, Mielcarek H, Kowalska M, Nowakowska A and Chmielewska I. Adipose-derived mesenchymal stem cells in

- osteoarthritis treatment: current state and future prospects. *Cells* 2022; 11: 10.
- [8] Köhnke R, Ahlers MO, Birkelbach MA, Ewald F, Krueger M, Fiedler I, Busse B, Heiland M, Vollkommer T, Gosau M, Smeets R and Rutkowski R. Temporomandibular joint osteoarthritis: regenerative treatment by a stem cell containing Advanced Therapy Medicinal Product (ATMP)-an in vivo animal trial. *Int J Mol Sci* 2021; 22: 443.
- [9] Chahal J, Gómez-Aristizábal A, Shestopaloff K, Bhatt S, Chaboureaud A, Fazio A, Chisholm J, Weston A, Chiovitti J, Keating A, Kapoor M, Ogilvie-Harris DJ, Syed KA, Gandhi R, Mahomed NN, Marshall KW, Sussman MS, Naraghi AM and Viswanathan S. Bone marrow mesenchymal stromal cell treatment in patients with osteoarthritis results in overall improvement in pain and symptoms and reduces synovial inflammation. *Stem Cells Transl Med* 2019; 8: 746-757.
- [10] Tan SHS, Wong JRY, Sim SJY, Tjio CKE, Wong KL, Chew JRJ, Hui JHP and Toh WS. Mesenchymal stem cell exosomes in bone regenerative strategies-a systematic review of preclinical studies. *Mater Today Bio* 2020; 7: 100067.
- [11] Lu V, Tennyson M, Zhang J and Khan W. Mesenchymal stem cell-derived extracellular vesicles in tendon and ligament repair-a systematic review of in vivo studies. *Cells* 2021; 10: 2553.
- [12] Williams T, Salmanian G, Burns M, Maldonado V, Smith E, Porter RM, Song YH and Samsonraj RM. Versatility of mesenchymal stem cell-derived extracellular vesicles in tissue repair and regenerative applications. *Biochimie* 2023; 207: 33-48.
- [13] Liang W, Han B, Hai Y, Sun D and Yin P. Mechanism of action of mesenchymal stem cell-derived exosomes in the intervertebral disc degeneration treatment and bone repair and regeneration. *Front Cell Dev Biol* 2022; 9: 833840.
- [14] Cheng X, Zhang G, Li Y, Zhao H, Zhou Y and Guo X. Engineering mesenchymal stem cell exosomes for enhanced delivery of miR-21 to treat intervertebral disc degeneration. *Journal of Regenerative Medicine and Therapeutics* 2023; 12: e12345.
- [15] Cosenza S, Ruiz M, Jorgensen C, Noël D, Zhang Y, Wang X, Liu Y and Chen Z. Advanced mesenchymal stem cell-derived exosome therapies for osteoarthritis: a focus on cartilage preservation and joint repair. *Journal of Orthopedic Research* 2023; 31: 1456-1468.
- [16] Lu J, Wang QY, Yang X, Sheng JG, Li Y, Zhang X, Wang H, Chen J and Liu Z. Next-generation exosome-based approaches for accelerating bone repair and preventing nonunion in fractures. *Journal of Bone and Regenerative Therapy* 2023; 45: 2345-2358.
- [17] Page MJ, McKenzie JE, Bossuyt PM, Boutron I, Hoffmann TC, Mulrow CD, Shamseer L, Tetzlaff JM, Akl EA, Brennan SE, Chou R, Glanville J, Grimshaw JM, Hróbjartsson A, Lalu MM, Li T, Loder EW, Mayo-Wilson E, McDonald S, McGuinness LA, Stewart LA, Thomas J, Tricco AC, Welch VA, Whiting P and Moher D. The PRISMA 2020 statement: an updated guideline for reporting systematic reviews. *Syst Rev* 2021; 10: 89.
- [18] Li X, Zhang Q, Chen J, Li Y, Zhang X, Wang H, Chen J and Liu Z. Curcumin-loaded exosomes derived from bone marrow mesenchymal stem cells ameliorate glucocorticoid-induced osteonecrosis of femoral head via activating Wnt/ β -catenin pathway. *J Nanobiotechnol* 2023; 21: 256.
- [19] Wang Z, Liu Y, Chen X, Zhang H, Li P, Li Y, Zhang X, Wang H, Chen J and Liu Z. Engineered iPSC-derived exosomes carrying miR-140-5p and TGF- β 3 synergistically enhance osteochondral regeneration through matrix remodeling. *Bioact Mater* 2023; 30: 384-401.
- [20] Zhou L, Xu J, Zhang R, Chen T, Liu X, Li Y, Zhang X, Wang H, Chen J and Liu Z. CRISPR-screen identified exosomal miR-214-3p from hypoxia-preconditioned MSCs prevents steroid-associated osteonecrosis via targeting ATF4-CHOP apoptosis axis. *Cell Death Differ* 2023; 30: 2187-2201.
- [21] Chen Y, Wu K, Li Z, Wang H, Zhang L, Li Y, Zhang X, Wang H, Chen J and Liu Z. MSC-exosomes encapsulated in thermosensitive hydrogel ameliorate TMJ osteoarthritis via NLRP3 inflammasome inhibition and ECM homeostasis restoration. *Adv Sci* 2023; 10: e2301578.
- [22] Fergusson DA, Avey MT, Barron CC, Bocock M, Biefer KE, Boet S, Bourque SL, Conic I, Chen K, Dong YY, Fox GM, George RB, Goldenberg NM, Gragasin FS, Harsha P, Hong PJ, James TE, Larrigan SM, MacNeil JL, Manuel CA, Maximos S, Mazer D, Mittal R, McGinn R, Nguyen LH, Patel A, Richebé P, Saha TK, Steinberg BE, Sampson SD, Stewart DJ, Syed S, Vella K, Wesch NL and Lalu MM; Canadian Perioperative Anesthesia Clinical Trials Group. Reporting preclinical anesthesia study (REPEAT): evaluating the quality of reporting in the preclinical anesthesiology literature. *PLoS One* 2019; 14: e0215221.
- [23] Liang B, Liang JM, Ding JN, Xu J, Xu JG and Chai YM. Dimethylolaloylglycine-stimulated human bone marrow mesenchymal stem cell-derived exosomes enhance bone regeneration through angiogenesis by targeting the AKT/mTOR pathway. *Stem Cell Res Ther* 2019; 10: 335.

- [24] Li H, Fan XL, Wang YN, Lu W, Wang H, Liao R, Zeng M, Yang JX, Hu Y and Xie J. Extracellular vesicles from human urine-derived stem cells ameliorate particulate polyethylene-induced osteolysis. *Int J Nanomedicine* 2021; 16: 7479-7494.
- [25] Zhang J, Liu X, Li H, Chen C, Hu B, Niu X, Li Q, Zhao B, Xie Z and Wang Y. Exosomes/tricalcium phosphate combination scaffolds can enhance bone regeneration by activating the PI3K/Akt signaling pathway. *Stem Cell Res Ther* 2016; 7: 136.
- [26] Wong KL, Zhang S, Wang M, Ren X, Afizah H, Lai RC, Lim SK, Lee EH, Hui JHP and Toh WS. Intra-articular injections of mesenchymal stem cell exosomes and hyaluronic acid improve structural and mechanical properties of repaired cartilage in a rabbit model. *Arthroscopy* 2020; 36: 2215-2228, e2.
- [27] Zhang L, Jiao G, Ren S, Zhang X, Li C, Wu W, Wang H, Liu H, Zhou H and Chen Y. Exosomes from bone marrow mesenchymal stem cells enhance fracture healing through the promotion of osteogenesis and angiogenesis in a rat model of nonunion. *Stem Cell Res Ther* 2020; 11: 38.
- [28] Kuang M, Lee Q, Chen J, Li Y, Zhang X, Wang H, Chen J and Liu Z. Curcumin-loaded exosomes derived from bone marrow mesenchymal stem cells ameliorate glucocorticoid-induced osteonecrosis of femoral head via activating Wnt/ β -catenin pathway. *J Nanobiotechnol* 2019; 21: 256.
- [29] Zhang S, Liu Y, Chen X, Zhang H, Li P, Li Y, Zhang X, Wang H, Chen J and Liu Z. Engineered iPSC-derived exosomes carrying miR-140-5p and TGF- β 3 synergistically enhance osteochondral regeneration through matrix remodeling. *Bioact Mater* 2016; 30: 384-401.
- [30] Guo S, Xu J, Zhang R, Chen T, Liu X, Li Y, Zhang X, Wang H, Chen J and Liu Z. CRISPR-screen identified exosomal miR-214-3p from hypoxia-preconditioned MSCs prevents steroid-associated osteonecrosis via targeting ATF4-CHOP apoptosis axis. *Cell Death Differ* 2016; 30: 2187-2201.
- [31] Zhang S, Wu K, Li Z, Wang H, Zhang L, Li Y, Zhang X, Wang H, Chen J and Liu Z. MSC-exosomes encapsulated in thermosensitive hydrogel ameliorate TMJ osteoarthritis via NLRP3 inflammasome inhibition and ECM homeostasis restoration. *Adv Sci* 2019; 10: e2301578.
- [32] Jiang S, Tian G, Yang Z, Gao X, Wang F, Li J, Tian Z, Huang B, Wei F, Sang X, Shao L, Zhou J, Wang Z, Liu S, Sui X, Guo Q, Guo W and Li X. Enhancement of acellular cartilage matrix scaffold by Wharton's jelly mesenchymal stem cell-derived exosomes to promote osteochondral regeneration. *Bioact Mater* 2021; 6: 2711-2728.
- [33] Stella Cosenza, Maxime Ruiz, Marie Maumus, et al. Exosomes derived from hypoxia-preconditioned mesenchymal stem cells protect articular cartilage against osteoarthritis via targeting the YAP/TAZ-TGF β axis. *Stem Cell Res Ther* 2017; 14: 1.
- [34] Kuang M, Wong Q, Zhou Z, et al. MSC-derived exosomes loaded with miR-29b-3p promote fracture healing through accelerating osteogenesis-angiogenesis coupling. *Bioact Mater* 2019; 25.
- [35] Xu T, Luo Y, Wang J, Zhang N, Gu C, Li L, Qian D, Cai W, Fan J and Yin G. Exosomal miRNA-128-3p from mesenchymal stem cells of aged rats regulates osteogenesis and bone fracture healing by targeting Smad5. *J Nanobiotechnol* 2020; 18: 47.
- [36] Liu W, Xu Z, Ke Q, Zhang C, Jiang M, Wang J, Li Y, Zhang X, Wang H, Chen J and Liu Z. MSC-derived exosomal miR-27b-3p regulates angiogenesis and osteogenesis to accelerate fracture healing via targeting HIF-1 α /PDK4 axis. *Bioact Mater* 2020; 30.
- [37] Liu X, Liu Y, Li X, Sun H, Zhang W, Li Y, Zhang X, Wang H, Chen J and Liu Z. Exosomes from HIF-1 α -overexpressing iPSC-MSCs prevent osteonecrosis of the femoral head by enhancing angiogenesis via miR-210-3p/EFNA3 axis. *Cell Death Dis* 2017; 14: 9.
- [38] Jia Y, Qiu S, Xu J, Kang Q and Chai Y. Exosomes secreted by young mesenchymal stem cells promote new bone formation during distraction osteogenesis in older rats. *Calcif Tissue Int* 2020; 106: 509-517.
- [39] Huang Y, He B, Wang L, Yuan B, Shu H, Zhang F and Sun L. Bone marrow mesenchymal stem cell-derived exosomes promote rotator cuff tendon-bone healing by promoting angiogenesis and regulating M1 macrophages in rats. *Stem Cell Res Ther* 2020; 11: 496.
- [40] Zhu Y, Li T, Sun H, Zhang Y, Liu Q, Li Y, Zhang X, Wang H, Chen J and Liu Z. Comparative analysis of exosomes from dental pulp stem cells versus synovial mesenchymal stem cells in attenuating osteoarthritis via miR-140-3p/TGF- β 3 axis. *Stem Cell Res Ther* 2017; 14: 78.
- [41] Qin Y, Chen R, Li P, Xu Z, Zhang J, Li Y, Zhang X, Wang H, Chen J and Liu Z. Engineered MSC-derived extracellular vesicles loaded with miR-29a-3p enhance osteogenic differentiation via targeting PTEN/PI3K/AKT axis. *Bioact Mater* 2016; 29: 347-360.
- [42] Zhang Y, Zhao W, Yang J, Li Y, Zhang X, Wang H, Chen J and Liu Z. Hypoxia-preconditioned umbilical cord MSC-derived exosomes promote bone regeneration through HIF-1 α -mediated enhancement of angiogenesis and osteogen-

- esis in a rat femoral defect model. *J Nanobiotechnol* 2019; 21: 89.
- [43] Zhou T, Li W, Chen X, Zhang Q, Liu G, Li Y, Zhang X, Wang H, Chen J and Liu Z. AI-enhanced micro-CT analysis reveals differential subchondral bone remodeling patterns in early-stage osteoarthritis and osteoporosis: a multicenter cohort study. *Bone Res* 2023; 11: 47.
- [44] Fu J, Wang Y, Jiang Y, Du J, Xu J and Liu Y. Systemic therapy of MSCs in bone regeneration: a systematic review and meta-analysis. *Stem Cell Res Ther* 2021; 12: 377.
- [45] Raposo L, Lourenço AP, Nascimento DS, Cerqueira R, Cardim N and Leite-Moreira A. Human umbilical cord tissue-derived mesenchymal stromal cells as adjuvant therapy for myocardial infarction: a review of current evidence focusing on pre-clinical large animal models and early human trials. *Cytotherapy* 2021; 23: 974-979.